

## Structure-Activity and Antioxidant Properties of Quercetin and Its Co<sup>2+</sup> Chelate

Fatih Yalcin <sup>1,\*</sup>, Asli Ozturk Kiraz <sup>1</sup>

<sup>1</sup>Pamukkale University, Faculty of Science and Letters, Department of Physics, Denizli, Turkiye

**Abstract:** Quercetin and its metal complexes have anti-oxidation, anti-bacterial, anti-tumor, and kinds of enzymatic activities. Studies in recent years, these activities are very important for health and pharmaceuticals. The purpose of this manuscript is to determine the structure-activity relations and antioxidant properties of the Quercetin and Quercetin-Co<sup>2+</sup> chelate from a theoretical view and to be used these compounds in the treatment of the diseases. We found that Quercetin is more stable than Quercetin-Co<sup>2+</sup> chelate but Quercetin-Co<sup>2+</sup> chelate is more conductive and the O22-H bond of the Quercetin molecule has the highest antioxidant activity. The remarkable electron delocalization occurred between the donor (C17-C19) anti bond and acceptor (C13-C15) anti bond with 319.62 kcal/mol stabilization energy in Quercetin.

### ARTICLE HISTORY

*Received:* June 29, 2021

*Revised:* Nov. 24, 2021

*Accepted:* Dec. 15, 2021

### KEYWORDS

Polyphenol compounds,  
Metal chelating activity,  
Electronic properties,  
Antioxidant activity

## 1. INTRODUCTION

Flavonoids are considerably available plant-derived polyphenol compounds with several biological and chemical activities. (Kasprzak *et al.*, 2015). Due to the hydroxyl groups in their structure flavonoids are demonstrated antioxidant properties and with the help of these groups, they can coordinate metal ions and form complexes (Symonowicz *et al.*, 2012). Metal complexes of flavonoids have several stimulating features: they are colored, often fluorescent, anti-oxidant or pro-oxidant, antimicrobial, antiproliferative, and biologically ascendant in numerous different manners.

Generally, the free radical scavenging properties of flavone compounds constitute their antioxidant mechanism. The other mechanism for antioxidant behavior may occur from interactions between flavonoids and transition metal ions, preventing the participation of metal ions in free radical formation processes (Mira *et al.*, 2002). Recent studies have shown that metal-flavonoid complexes have favorable biological and pharmacological activities and some of them have been used successfully in clinical applications (Grazul *et al.*, 2009; Afanas'eva *et al.*, 2001).

\*CONTACT: Fatih Yalcin ✉ [fatihyalcin6635@gmail.com](mailto:fatihyalcin6635@gmail.com) 📍 Pamukkale University, Faculty of Science and Letters, Department of Physics, 20070, Denizli, Turkiye

Quercetin (3,3',4',5,7-pentahydroxyflavone) is one of the most bioactive and prevalent nutritional flavonoids, which is widely found in the flowers, leaves, and fruits of many plants (Chen *et al.*, 2009; Bravo *et al.*, 2001). It has been notified that quercetin coincides with complexes with transition metal ions, such as  $\text{Cu}^{2+}$ ,  $\text{Mn}^{2+}$ , and  $\text{Fe}^{2+}$ . Quercetin and its chelating activity with  $\text{Cu}^{2+}$ ,  $\text{Mn}^{2+}$ , and  $\text{Fe}^{2+}$  reveal wide biological activities with increasing bioavailability, such as anti-oxidation, anti-bacterial, anti-tumor, and the talent to impress many kinds of enzymatic activities (Zhou *et al.*, 2001; Mendoza *et al.*, 2011). These quercetin/metallic ion complexes not only improve its bioavailability and alter the *in vivo* delivery route of quercetin but also encourage new pharmacological activity (Malesev *et al.*, 2007; Cornard *et al.*, 2002; Yamashita *et al.*, 1999).

In the literature, many papers cover specific aspects of the activity of flavonoid metal complexes, e.g. their antioxidant properties, enzyme-mimicking behavior, therapeutic potential, or use in chemical analysis. Furthermore, we need to know the physical properties of metal complexes of flavonoids as well as chemical properties. There are five antioxidant mechanisms we have explained previously in our article (Kiraz 2019; Torreggiani *et al.*, 2005; El Hajji *et al.*, 2006; Leopoldini *et al.*, 2006; Xu *et al.*, 2007; Jurasekova *et al.*, 2009; Dehghan *et al.*, 2011; Dolatabadi, 2011; Zhang *et al.*, 2011).

In this study, we have utilized the B3LYP/6-31++G(d,p) method to explore the antioxidant effects and structure-activity relationships of quercetin chelate with  $\text{Co}^{2+}$ . The electronic properties and various molecular descriptors such as the bond dissociation enthalpy (BDE), adiabatic ionization potential (AIP) of the chelate complexes have also been obtained and studied, which are relevant to show evidence of antioxidant activity.

## 2. MATERIAL and METHODS

Hybrid density functional theory (DFT) is one of the most successful quantum chemistry tools in describing the ground state and excited properties of metal complexes of flavonoids. The most popular DFT method is B3LYP (Becke3-Parameter method for calculating that part of the molecular energy due to overlapping orbitals plus the Lee-Yang-Parr method of accounting for correlation) (Tachibana *et al.*, 2002; Pai *et al.*, 2006; Zade *et al.*, 2006).

The molecular structure of the compound was optimized to get the global minima by using the B3LYP/6-31++G(d,p) level. In this study, geometric parameters (bond lengths and bond angles), the highest occupied molecular orbital (HOMO) energies, the lowest unoccupied molecular orbital (LUMO) energies, the electronic properties (total energy, dipole moment, electronegativity, chemical hardness, and softness), optical properties of a compound formed by  $\text{Co}^{2+}$  and flavonoid have been performed by using Gaussian 16 (Frisch *et al.*, 2016) and GaussView 6.0 (Dennigton *et al.*, 2016) was used for visualization of the structure. We calculated the probability of transitions between a ground state and excited states by using time-dependent density functional theory (TD-DFT). The major contribution rate of HOMO–LUMO orbitals is determined by using the GaussSum 2.2 program (Joseph *et al.*, 2014).

## 3. RESULTS / FINDINGS

To examine the electronic and antioxidant properties, it is necessary to know the most stable state of Quercetin and Quercetin- $\text{Co}^{2+}$  chelate. These calculated structures (Yalçın, 2019) are shown in [Figure 1](#) and [Figure 2](#).

**Figure 1.** Optimized geometry of Quercetin.

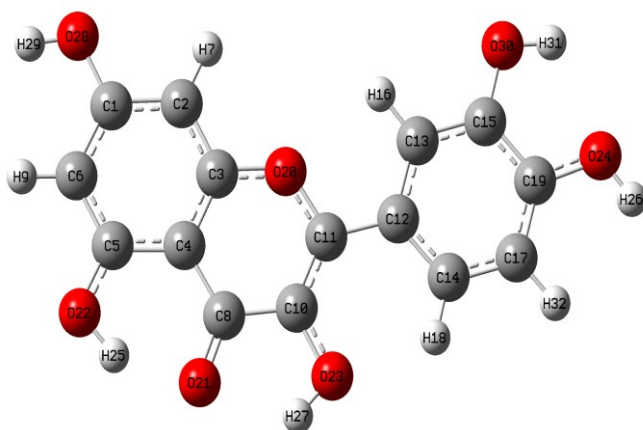
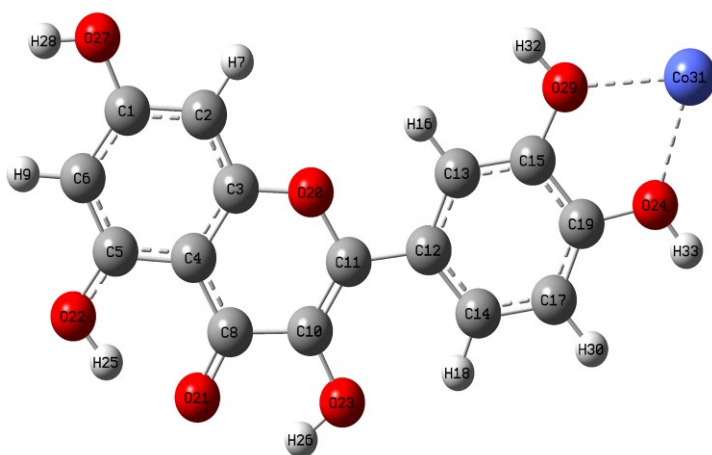


**Figure 2.** Optimized geometry of Quercetin chelate with  $\text{Co}^{2+}$ .



### 3.1. Electronic Properties

Electronic parameters of Quercetin and Quercetin- $\text{Co}^{2+}$  chelate are presented in Table 1 (Yalçın, 2019). Since HOMO-LUMO energy difference ( $\Delta E$ ) represents the chemical reactivity of a molecule.

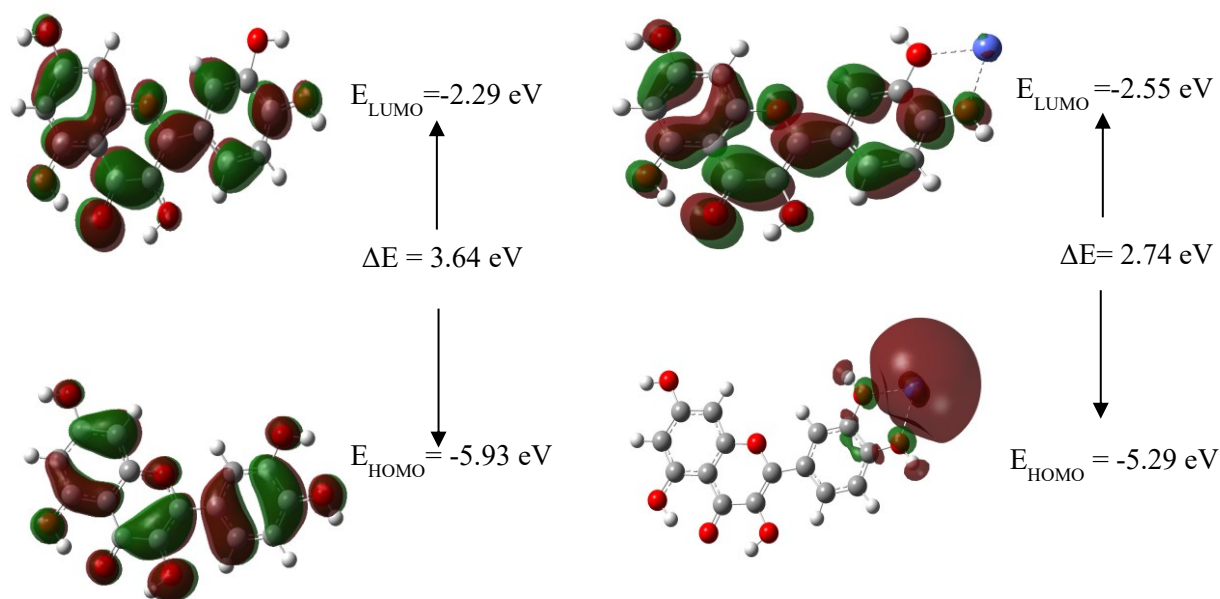
**Table 1.** Molecular descriptors of Quercetin and Quercetin- $\text{Co}^{2+}$  chelate calculated at B3LYP/6-31++G(d,p) level.

Parameters	Quercetin	Quercetin- $\text{Co}^{2+}$
$E_{\text{LUMO}}$ (eV)	-2.29	-2.55
$E_{\text{HOMO}}$ (eV)	-5.93	-5.29
$\Delta E = E_{\text{LUMO}} - E_{\text{HOMO}}$ (eV)	3.64	2.74
I (ionization potential) (eV)	5.93	5.29
A (electron affinity) (eV)	2.29	2.55
$\chi$ (electronegativity) (eV)	4.11	3.92
$\eta$ (global hardness) (eV)	1.82	1.37
S (global softness) ( $\text{eV}^{-1}$ )	0.55	0.73
$\mu$ (electronic chemical potential) (eV)	-4.11	-3.92
$\omega$ (global electrophilicity index) (eV)	4.64	5.60

As seen from Table 1, the energy difference between HOMO and LUMO orbitals of Quercetin and Quercetin-Co<sup>2+</sup> chelate are 3.64 and 2.74 eV, respectively. According to these  $\Delta E$  values, Quercetin -Co<sup>2+</sup> chelate is more conductive than Quercetin but the other parameters are quite close to each other. Especially, when we examine the global hardness and softness values of the molecules, the higher global hardness values are the evidence of the low reactivity of the molecule.

Figure 3. Molecular orbitals compositions of Quercetin.

Figure 4. Molecular orbitals compositions of Quercetin-Co<sup>2+</sup> chelate.



As seen from Figure 3; HOMO and LUMO orbitals are distributed throughout the Quercetin molecule. The LUMO orbitals are spread over the whole molecule while the HOMO orbitals are on Co<sup>2+</sup> seen in Figure 4.

TD-DFT calculations in the gas phase were carried out on Quercetin and Quercetin-Co<sup>2+</sup> put account B3LYP/6-31++G(d,p) functional to understand the electronic transitions of the compounds. Table 2 shows the electronic transitions, major contributions, calculated absorption peaks ( $\lambda_{\text{max}}$ 's), excitation energies, oscillator strengths (f), and assignments of the transitions of the Quercetin and Quercetin-Co<sup>2+</sup> molecules.

The electronic absorption peak (at 373 nm for Quercetin and 4565 nm for Quercetin-Co<sup>2+</sup>) corresponds to the transition from the ground state to the first excited state, which corresponds to HOMO to LUMO excitation with high oscillator strengths. This band arises from an  $n \rightarrow \pi^*$  transition (Kiraz, 2020). The second absorption band at 330 nm arises from HOMO-1 to LUMO transition for Quercetin and at 4193 nm arise from HOMO-2 to LUMO+12 for Quercetin-Co<sup>2+</sup>. However, the oscillator strength for the second transition is lower than the first transition for Quercetin and 0 for all the transitions of the Quercetin-Co<sup>2+</sup>. The third absorption peak at 305 nm for Quercetin arises from HOMO-2 to LUMO and the 2810 nm peak for Quercetin-Co<sup>2+</sup> arises from HOMO to LUMO excitation. Also, for the Quercetin, the oscillator strength for the second transition is lower than the third transition.

**Table 2.** Calculated absorption wavelengths, energies, and oscillator strengths of quercetin and quercetin-Co<sup>2+</sup> using the TD-DFT method at the B3LYP/6-31++G(d,p) level.

Quercetin					Quercetin-Co <sup>2+</sup>				
Excitation Major Cont.	CI expansion coefficient	WL Calc. gas phase (nm)	Excitation Energy (eV)	Osc. Str. (f)	Excitation	CI expansion coefficient	WL Calc. Water (nm)	Excitation Energy (eV)	Osc. Str. (f)
Excited State 1					Excited State 1				
Singlet-A					Singlet-A				
77 → 79 (3%) (HOMO-1 → LUMO)	0.12996	373.16	4.99	0.4253	90B → 104B (50%) HOMO-1 → LUMO + 12	-0.70437	4565.32	0.27	0.0000
78 → 79 (93%) (HOMO → LUMO)	0.68078				90B → 108B (29%) HOMO-1 → LUMO + 16	-0.05248			
Excited State 2					Excited State 2				
77 → 79 (94%) (HOMO-1 → LUMO)	0.68399	330.26	4.06	0.0853	89B → 104 (47%) HOMO-2 → LUMO + 12	0.68673	4193.09	0.30	0.0000
78 → 79 (3%) (HOMO → LUMO)	-0.13194				89B → 105B (27%) HOMO-2 → LUMO + 16	-0.22732			
Excited State 3					Excited State 3				
76 → 79 (90%) HOMO-2 → LUMO	0.66933	304.89	4.07	0.0980	91B → 92B (99%) HOMO → LUMO	0.99553	2809.92	0.44	0.0000
78 → 82 (5%) HOMO → LUMO + 3	0.16101								

### 3.2. Antioxidant Properties

For the antioxidant property; the significant parameters are bond dissociation enthalpy (BDE) which is associated with hydrogen atom transfer (HAT) mechanism and adiabatic ionization potential (AIP) which is related to the single electron transfer (SET) mechanism. These parameters are acquired by donating a hydrogen atom or single electron from the OH bonds (Leopoldini *et al.*, 2011). The lower BDE value remarks the better antioxidant activity of the molecule (Urbaniak *et al.*, 2012).

**Table 3.** Antioxidant Parameters of Quercetin and Quercetin-Co<sup>+2</sup> chelate.

Antioxidant Parameters	Quercetin		Quercetin-Co <sup>+2</sup>	
	O22 – H	O23 – H	O22 – H	O23 – H
BDE (kcal/mol)	393.78	398.31	442.82	429.51
AIP (kcal/mol)	166.36	166.36	158.68	158.68
PDE (kcal/mol)	-32.15	-27.61	24.58	11.28
PA (kcal/mol)	72.17	62.51	183.26	65.37
ETE (kcal/mol)	62.05	76.23	109.90	104.58

According to [Table 3](#), calculated BDE values in the gas phase specify that the O22-H bond of the Quercetin molecule has the highest antioxidant activity while the O22-H bond of the Quercetin-Co<sup>2+</sup> chelate is the lowest antioxidant capacity.

Proton dissociation enthalpy (PDE) with the AIP are also important parameters for the antioxidant capacity. The low value of the PDE parameter express that a single electron transfer followed by a proton transfer (SET-PT) mechanism is energetically chosen for the antioxidant activity (Kiraz, 2019). For the calculated values of PDE, the O22-H bond of the Quercetin has much more antioxidant activity than the O22-H bond of the Quercetin-Co<sup>2+</sup> chelate.

The sequential proton loss electron transfer (SPLET) mechanism is another significant antioxidant mechanism in which antioxidants grab free radicals and also the radical scavenging activity of a molecule can be assayed with this mechanism (Urbaniak *et al.*, 2012). For this mechanism, the proton affinity (PA) and electron transfer enthalpy (ETE) parameters are very substantial. The O23-H bond of the Quercetin has the lowest PA value and the O22-H bond of the Quercetin has the lowest ETE value. Therefore, the SPLET mechanism is not preferred for the antioxidant activity for Quercetin and Quercetin-Co<sup>2+</sup> chelate.

### 3.3. NBO Analysis

Natural Bond Orbitals (NBO) analysis is a remarkable method to determine intra and intermolecular bonding and charge a transfer or conjugative interaction in molecular systems (Tomasi *et al.*, 2005). The second-order Fock matrix was executed to utilize the donor-acceptor interactions (Snehalatha *et al.*, 2009). The significant element of the Fock matrix is the stabilization energy E<sup>(2)</sup> associated with the delocalization and a greater E<sup>(2)</sup> value presented the donating inclination from electron donors to electron acceptors.

The NBO analysis expresses conspicuous donor-acceptor type delocalization from lone-pair (LP) of oxygen orbitals with anti-lone-pair (LP\*) of a metal orbital. The delocalization effects because of the LP-LP\* interactions in the molecule play an excessively conspicuous task on the coordination environments of the Co<sup>2+</sup> ion (Kiraz, 2017). As seen from [Table 4](#); the significant

interactions of Quercetin compound are  $\pi^*(\text{C8-O21}) \rightarrow \pi^*(\text{C3-C4})$ ,  $\pi^*(\text{C10-C11}) \rightarrow \pi^*(\text{C12-C14})$ ,  $\pi^*(\text{C3-C4}) \rightarrow \pi^*(\text{C5-C6})$ ,  $\pi^*(\text{C17-C19}) \rightarrow \pi^*(\text{C12-C14})$ ,  $\pi^*(\text{C17-C19}) \rightarrow \pi^*(\text{C13-C15})$  which have stabilization energies 214.33, 201.67, 313.25, 319.62 and 298.96 kcal/mol, respectively (Yalçın, 2019).

**Table 4.** Second-order perturbation energies  $E^2$  (kcal/mol) corresponding to the most important charge transfer interaction (donor-acceptor) in Quercetin by DFT/B3LYP/6-31++G(d,p) method.

Donor	Type	ED/e	Acceptor	Type	ED/e	$E^2$ (kcal/mol)
C1-C2	$\pi$	1.66161	C3-C4	$\pi^*$	0.49121	29.19
			C5-C6	$\pi^*$	0.36994	12.49
C3-C4	$\pi$	1.62687	C1-C2	$\pi^*$	0.40740	12.42
			C5-C6	$\pi^*$	0.36994	24.69
			C8-O21	$\pi^*$	0.41495	34.97
C5-C6	$\pi$	1.69283	C1-C2	$\pi^*$	0.40740	27.93
			C3-C4	$\pi^*$	0.49121	12.20
C10-C11	$\pi$	1.76811	C8-O21	$\pi^*$	0.31363	24.61
			C12-C14	$\pi^*$	0.40886	10.63
C12-C14	$\pi$	1.64600	C10-C11	$\pi^*$	0.31363	17.65
			C13-C15	$\pi^*$	0.35887	19.64
			C17-C19	$\pi^*$	0.02505	19.56
C13-C15	$\pi$	1.67621	C12-C14	$\pi^*$	0.40886	18.30
			C17-C19	$\pi^*$	0.40455	20.52
C17-C19	$\pi$	1.68530	C12-C14	$\pi^*$	0.40886	19.45
			C13-C15	$\pi^*$	0.35887	18.05
O20	LP2	1.75006	C3-C4	$\pi^*$	0.49121	30.68
			C10-C11	$\pi^*$	0.31363	27.91
O21	LP2	1.85643	C4-C8	$\sigma^*$	0.04909	12.13
			C8-C10	$\sigma^*$	0.06078	15.98
			O22-H25	$\sigma^*$	0.05798	17.20
O22	LP2	1.81463	C5-C6	$\pi^*$	0.36994	39.67
O23	LP2	1.86352	C10-C11	$\pi^*$	0.31363	31.40
O24	LP2	1.88412	C17-C19	$\pi^*$	0.40455	25.89
O28	LP2	1.85642	C1-C2	$\pi^*$	0.40740	30.75
<b>C3-C4</b>	<b><math>\pi^*</math></b>	<b>0.49121</b>	<b>C5-C6</b>	<b><math>\pi^*</math></b>	<b>0.36994</b>	<b>313.25</b>
<b>C8-O21</b>	<b><math>\pi^*</math></b>	<b>0.41495</b>	<b>C3-C4</b>	<b><math>\pi^*</math></b>	<b>0.49121</b>	<b>214.33</b>
			C10-C11	$\pi^*$	0.31363	107.82
<b>C10-C11</b>	<b><math>\pi^*</math></b>	<b>0.31363</b>	<b>C12-C14</b>	<b><math>\pi^*</math></b>	<b>0.40886</b>	<b>201.67</b>
<b>C17-C19</b>	<b><math>\pi^*</math></b>	<b>0.40455</b>	<b>C12-C14</b>	<b><math>\pi^*</math></b>	<b>0.40886</b>	<b>319.62</b>
			<b>C13-C15</b>	<b><math>\pi^*</math></b>	<b>0.35887</b>	<b>298.96</b>



**Table 5.** Second-order perturbation energies  $E^2$  (kcal/mol) corresponding to the most important charge transfer interaction (donor-acceptor) in Quercetin- $\text{Co}^{2+}$  by DFT/B3LYP/6-31++G(d,p) method.

Donor	Type	ED/e	Acceptor	Type	ED/e	$E^2$ (kcal/mol)	
C1-C2	$\pi$	0.83323	C3-C4	$\pi^*$	0.24413	14.39	
C3-C4	$\pi$	0.81404	C5-C6	$\pi^*$	0.18601	12.45	
			C8-O21	$\pi^*$	0.20990	17.29	
C5-C6	$\pi$	0.84687	C1-C2	$\pi^*$	0.20380	13.98	
C10-C11	$\pi$	0.88069	C8-O21	$\pi^*$	0.20990	12.59	
<b>C19</b>	<b>LP1</b>	<b>0.50954</b>	<b>C14-C17</b>	<b><math>\sigma^*</math></b>	<b>0.00631</b>	<b>31.33</b>	
O20	LP2	0.87479	C3-C4	$\pi^*$	0.24413	15.48	
			C10-C11	$\pi^*$	0.15911	13.80	
O22	LP1	0.90750	C5-C6	$\pi^*$	0.18601	19.85	
O23	LP2	0.93154	C10-C11	$\pi^*$	0.15911	15.67	
O27	LP2	0.92933	C1-C2	$\pi^*$	0.20380	15.23	
			C13-C15	$\sigma^*$	0.01370	0.03	
			C17-C19	$\sigma^*$	0.01456	0.03	
	Co31	LP1	0.99873	C19-O24	$\sigma^*$	0.01315	0.11
				C13-C15	$\sigma^*$	0.01370	0.15
				C15-O29	$\sigma^*$	0.01164	0.14
				C17-C19	$\sigma^*$	0.01456	0.15
LP3	0.99508	C19-O24	$\sigma^*$	0.01315	0.40		

The most important interaction for the Quercetin- $\text{Co}^{2+}$  chelate is the LP1(C19)  $\rightarrow$   $\sigma^*$ (C14-C17) with the stabilization energy of 31.33 kcal/mol. The other interactions are generally  $\pi^*$  orbitals between C-C bonds. From Table 5; LP2 (20)  $\rightarrow$   $\pi^*$ (C3-C4), LP2 (O22)  $\rightarrow$   $\pi^*$ (C5-C6), and LP (O23)  $\rightarrow$   $\pi^*$ (C10-C11) have stabilization energies are 15.48, 19.85, and 15.67 kcal/mol, respectively.

#### 4. DISCUSSION and CONCLUSION

In this study, we have compared the electronic and antioxidant properties of the Quercetin and Quercetin- $\text{Co}^{2+}$  chelate. The energy values of HOMO-LUMO orbitals present that the Quercetin- $\text{Co}^{2+}$  chelate is more kinetically reactive than the Quercetin molecule. The absorption peaks with non-negligible oscillator strengths for Quercetin at a longer wavelength of 305~373 nm compared with those for the Quercetin- $\text{Co}^{2+}$  chelate at 4600~2800 nm. For the antioxidant capacity, the O22-H bond of the Quercetin molecule has the highest antioxidant activity which prefers the SET-PT antioxidant mechanism. The important electron delocalization was observed between the donor (C17-C19) anti bond and acceptor (C13-C15) anti bond with the stabilization energy 319.62 kcal/mol in Quercetin. The highest antioxidant property was observed in the Quercetin molecule where the highest electron delocalizations occurred.

#### Acknowledgments

The authors are grateful to Pamukkale University (Grant no: 2018FEBE002) and TUBITAK ULAKBIM, High Performance and Grid Computing Center (TRUBA Resources).

#### Declaration of Conflicting Interests and Ethics

The authors declare no conflict of interest. This research study complies with research and publishing ethics. The scientific and legal responsibility for manuscripts published in IJSM belongs to the authors.



### Authorship contribution statement

Authors are expected to present author contributions statement to their manuscript such as; **Fatih Yalcin**: Investigation, Resources, Software, Formal Analysis, Writing Original Draft. **Asli Ozturk Kiraz**: Methodology, Supervision, Visualization, Formal Analysis, Writing Original Draft, and Validation.

### Orcid

Fatih Yalcin  <https://orcid.org/0000-0002-8239-989X>

Asli Ozturk Kiraz  <https://orcid.org/0000-0001-9837-0779>

### 5. REFERENCES

- Afanas'eva, I.B., Ostrakhovitch, E.A., Mikhal'chik, E.V., Ibragimova, G.A., & Korkina, L.G. (2001). Enhancement of antioxidant and anti-inflammatory activities of bioflavonoid rutin by complexation with transition metals. *Biochem. Pharmacol.*, *61*, 677–684. [https://doi.org/10.1016/s0006-2952\(01\)00526-3](https://doi.org/10.1016/s0006-2952(01)00526-3)
- Bravo, A., & Anaconda, J.R. (2001). Metal complexes of the flavonoid quercetin: Antibacterial properties. *Transit. Metal Chem.*, *26*, 20–23. <https://doi.org/10.3390/molecules20058583>
- Chen, W.J., Sun, S.F., Cao, W., Liang, Y., & Song, J.R. (2009). The antioxidant property of quercetin Cr (III) complex: The role of Cr(III) ion. *J. Mol. Struct.*, *918*, 194–197. <https://doi.org/10.15171/bi.2019.15>
- Cornard, J.P., & Merlin, J.C. (2002). Spectroscopic and structural study of complexes of quercetin with Al (III). *J. Inorg. Biochem.*, *92*, 19–27. [https://doi.org/10.1016/s0162-0134\(02\)00469-5](https://doi.org/10.1016/s0162-0134(02)00469-5)
- Dehghan, G., Dolatabadi, J.E.N., Jouyban, A., Zeynali, K.A., Ahmadi, S.M., & Kashanian, S. (2011). Spectroscopic Studies on the Interaction of Quercetin-Terbium(III) Complex with Calf Thymus DNA. *DNA Cell Biol.*, *30*, 195–201. <https://doi.org/10.1089/dna.2010.1063>
- Dennington, R., Keith, T. A., & Millam, J. M. (2016). GaussView, Version 6, Copyright Semichem, Inc.
- Dolatabadi, J.E.N. (2011). Molecular aspects on the interaction of quercetin and its metal complexes with DNA. *Int. J. Biol. Macromol.*, *48*, 227-233. <https://doi.org/10.1016/j.ijbio mac.2010.11.012>
- El Hajji, H., Nkhili, E., Tomao, V., Dangles, O. (2006). Interactions of quercetin with iron and copper ions: Complexation and autoxidation. *Free Radic. Res.*, *40*, 303–320. <https://doi.org/10.1080/10715760500484351>
- Frisch, M. J., Trucks, G. W., Schlegel, H. B., Scuseria, G. E., Robb, M. A., Cheeseman, J. R., Scalmani, G., Barone, V., Petersson, G. A., Nakatsuji, H., Li, X., Caricato, M., Marenich, A. V., Bloino, J., Janesko, B. G., Gomperts, R., Mennucci, B., Hratchian, H. P., Ortiz, J. V., Izmaylov, A. F., Sonnenberg, J. L., Williams-Young, D., Ding, F., Lipparini, F., Egidi, F., Goings, J., Peng, B., Petrone, A., Henderson, T., Ranasinghe, D., Zakrzewski, V. G., Gao, J., Rega, N., Zheng, G., Liang, W., Hada, M., Ehara, M., Toyota, K., Fukuda, R., Hasegawa, J., Ishida, M., Nakajima, T., Honda, Y., Kitao, O., Nakai, H., Vreven, T., Throssell, K., Montgomery, J. A., Jr., Peralta, J. E., Ogliaro, F., Bearpark, M. J., Heyd, J. J., Brothers, E. N., Kudin, K. N., Staroverov, V. N., Keith, T. A., Kobayashi, R., Normand, J., Raghavachari, K., Rendell, A. P., Burant, J. C., Iyengar, S. S., Tomasi, J., Cossi, M., Millam, J. M., Klene, M., Adamo, C., Cammi, R., Ochterski, J. W., Martin, R. L., Morokuma, K., Farkas, O., Foresman, J. B., & Fox, D. J. (2016). Gaussian 16, Revision C.01, Gaussian, Inc., Wallingford CT.
- Grazul, M., & Budzisz, E. (2009). Biological activity of metal ions complexes of chromones, coumarins, and flavones. *Coord. Chem. Rev.*, *253*, 2588-2598. <https://doi.org/10.1016/j.ccr.2009.06015>

- Joseph, L., Sajan, D., Chaitanya K., Suthan T., Rajesh, N.P., & Isaac J. (2014). Molecular structure, NBO analysis, electronic absorption, and vibrational spectral analysis of 2-Hydroxy-4-Methoxybenzophenone: Reassignment of fundamental modes. *Spectrochim Acta A: Mol Biomol Spectrosc.*, 120, 216. <https://doi.org/10.1016/j.saa.2013.09.128>
- Jurasekova, Z., Torreggiani, A., Tamba, M., Sanchez-Cortes, S., & Garcia-Ramos, J.V. (2009). Raman and surface-enhanced Raman scattering (SERS) investigation of the quercetin interaction with metals: Evidence of structural changing processes in aqueous solution and on metal nanoparticles. *J. Mol. Struct.*, 918, 129-137. <https://doi.org/10.1016/j.molstruc.2008.07.025>
- Kasprzak, M. M., Erxleben, A., & Ochock, J. (2015). Properties and applications of flavonoid metal complexes. *RSC Advances*, 5, 45853-45877. <https://doi.org/10.1039/C5RA05069C>
- Kiraz, A. Ö., & Kaya, S. (2017). Structural and electrical properties of the Ca(PO<sub>4</sub>)<sub>2</sub> compound. *Physical Sciences (NWSAPS) 12(1)*, 8-21. <https://doi.org/10.12739/NWSA.2017.12.2.3A0079>
- Kiraz, A. Ö. (2019). Temperature Effect of the Theobromine's electronic and antioxidant properties. *Int. J. Sec. Metabolite*, 6(1), 90-97. <https://doi.org/10.21448/ijsm.504474>
- Kiraz, Aslı Öztürk, (2020). Theoretical insight into the antioxidant, electronic and anticancer behavior of *simmondsin*. *IJBB*, 57, 530-538.
- Leopoldini, M., Russo, N., Chiodo, S., & Toscano, M. (2006). Iron chelation by the powerful antioxidant flavonoid quercetin. *J. Agric. Food Chem.*, 54, 6343-6351. <https://doi.org/10.1021/jf060986h>
- Leopoldini, M., Russo, N., & Toscano M. (2011). The molecular basis of the working mechanism of natural polyphenolic antioxidants. *Food Chemistry*, 125, 288–306. <https://doi.org/10.1016/j.foodchem.2010.08.012>
- Malesev, D., & Kuntic, V. (2007). Investigation of metal-flavonoid chelates and the determination of flavonoids via metal-flavonoid complexing reactions. *J. Serb. Chem. Soc.*, 72, 921–939. <https://doi.org/10.2298/JSC0710921M>
- Mendoza, E.E. & Burd, R. (2011). Quercetin as a Systemic Chemopreventative Agent: Structural and Functional Mechanisms. *Mini-Rev. Med. Chem.*, 11, 1216–1221. <https://doi.org/10.2174/13895575111091216>
- Mira, L., Fernandez, M.T., Santos, M., Rocha, R., Florencio, M.H., & Jennings, K.R. (2002). Interactions of flavonoids with iron and copper ions: A mechanism for their antioxidant activity. *Free Radic. Res.*, 36, 1199–208. <https://doi.org/10.1080/1071576021000016463>
- Pai, C.L., Liu C.L., Chen, W.C., & Jenekhe, S. A. (2006). Electronic structure and properties of alternating donor-acceptor conjugated copolymers: 3,4-Ethylenedioxythiophene (EDOT) copolymers and model compounds. *Polymer*, 47, 699 – 708. <https://doi.org/10.1016/j.polymer.2005.11.083>
- Snehalatha, M., Ravikumar, C., Joe, I., Sekar, N., & Jayajumar, V.S. (2009). Spectroscopic analysis and DFT calculations of a food additive carmoisine. *Spectrochim Acta A: Mol Biomol Spectrosc.*, 72, 654–662. <https://doi.org/10.1016/j.saa.2008.11.017>
- Symonowicz, M., & Kolanek, M. (2012). Flavonoids and their properties to form chelate complexes. *Biotechnol Food Sci.*, 76 (1), 35-41.
- Tachibana M., Tanaka, S., Yamashita, Y., & Yoshizawa, K. (2002). Small Band-Gap Polymers Involving Tricyclic Nonclassical Thiophene as a Building Block. *J. Phys. Chem. B*, 106, (14), 3549–3556. <https://doi.org/10.1021/jp0115906>
- Tomasi, J., Mennucci, B., & Cammi, R. (2005). Quantum Mechanical Continuum Solvation Models. *Chem. Rev.*, 105(8), 2999–3094. <https://doi.org/10.1021/cr9904009>
- Torreggiani, A., Tamba, M., Trincherro, A., Bonora, S. (2005). Copper(II)-quercetin complexes in aqueous solutions: Spectroscopic and kinetic properties. *J. Mol. Struct.*, 744, 759-766. <https://doi.org/10.1016/j.molstruc.2004.11.081>

- Urbaniak, A., Molski, M., & Szelaĝ, M. (2012). Quantum-chemical Calculations of the Antioxidant Properties of trans-p-coumaric Acid and trans-sinapinic Acid. *CMST*, 18(2) 117-128. <https://doi.org/10.12921/cmst.2012.18.02.117-128>
- Xu, G.R., In, Y.M., Yuan, Y., Lee, J.J., & Kim, S. (2007). In situ spectroelectrochemical study of quercetin oxidation and complexation with metal ions in acidic solutions. *Bull. Korean Chem. Soc.*, 28, 889–892. <https://doi.org/10.5012/bkcs.2007.28.5.889>
- Yalçın, F. (2019). [Theoretical Investigation of the Interactions Between Some Flavonoid Molecules and Metal Ions]. [Master Thesis, Pamukkale University].
- Yamashita, N., Tanemura, H., & Kawanishi, S. (1999). Mechanism of oxidative DNA damage induced by quercetin in the presence of Cu (II). *Mutat. Res.*, 425, 107–115. [https://doi.org/10.1016/s0027-5107\(99\)00029-9](https://doi.org/10.1016/s0027-5107(99)00029-9)
- Zade, S.S., & Bendikov, M. (2006). From Oligomers to Polymer: Convergence in the HOMO–LUMO Gaps of Conjugated Oligomers. *Org. Lett.*, 8, 5243 - 5246. <https://doi.org/10.1021/ol062030y>
- Zhang, Y.P., Shi, S.Y., Sun, X.R., Xiong, X., & Peng, M.J. (2011). The effect of Cu<sup>2+</sup> on the interaction between flavonoids with different C-ring substituents and bovine serum albumin: Structure-affinity relationship aspect. *J. Inorg. Biochem.*, 105, 1529–1537. <https://doi.org/10.1016/j.jinorgbio.2011.08.007>
- Zhou, J., Wang, L.F., Wang, J.Y., & Tang, N. (2001). Antioxidative and anti-tumor activities of solid quercetin metal (II) complexes. *Transit. Metal Chem.*, 26, 57–63. [https://doi.org/10.1016/S0162-0134\(00\)00128-8](https://doi.org/10.1016/S0162-0134(00)00128-8)